

## Vapor Permeation Characteristics of TiO<sub>2</sub> Composite Membranes Prepared on Porous Stainless Steel Support by Sol-Gel Method

Yoon-Gyu Lee,<sup>†,‡</sup> Dong-Wook Lee,<sup>†</sup> Sang-Kyoon Kim,<sup>†</sup> Bongkuk Sea,<sup>†</sup>  
Min-Young Youn,<sup>†</sup> Kwan-Young Lee,<sup>‡</sup> and Kew-Ho Lee<sup>†,\*</sup>

<sup>†</sup>Membrane and Separation Research Center, Korea Research Institute of Chemical Technology (KRICT),  
P.O. Box 107, Yusong, Daejeon 305-606, Korea

<sup>‡</sup>Catalysis and Reaction Engineering Lab, Department of Chemical Engineering, Korea University, Seoul 136-701, Korea  
Received July 18, 2003

Composite membranes with a titania layer were prepared by soaking-rolling method with the titania sol of nanoparticles formed in the sol-gel process and investigated regarding the vapor permeation of various organic mixtures. The support modification was conducted by pressing SiO<sub>2</sub> xerogel of 500 nm in particle size under 10 MPa on the surface of a porous stainless steel (SUS) substrate and designed the multi-layered structure by coating the intermediate layer of  $\gamma$ -Al<sub>2</sub>O<sub>3</sub>. Microstructure of titania membrane was affected by heat-treatment and synthesis conditions of precursor sol, and titania formed at calcination temperature of 300 °C with sol of [H<sup>+</sup>]/[TIP]=0.3 possessed surface area of 210 m<sup>2</sup>/g, average pore size of 1.25 nm. The titania composite membrane showed high H<sub>2</sub>/N<sub>2</sub> selectivity and water/ethanol selectivity as 25-30 and 50-100, respectively. As a result of vapor permeation for water-alcohol and alcohol-alcohol mixture, titania composite membrane showed water-permselective and molecular-sieve permeation behavior. However, water/methanol selectivity of the membrane was very low because of chemical affinity of permeants for the membrane by similar physicochemical properties of water and methanol.

**Key Words :** Membrane separation, Titania, Sol-gel process, Vapor permeation, Dehydration

### Introduction

Ceramic membranes have received significant attention in recent years because of their excellent characteristics, such as chemical resistance, mechanical strength and thermal stability. Especially, microporous ceramic membranes with high selectivity and enhanced stability at high temperatures are very attractive systems for gas separation.<sup>1-4</sup> In addition, the application of ceramic membranes in so-called membrane reactors has been very promising from the viewpoint of size reduction as well as energy saving of chemical processes in the past few years.<sup>5</sup> When the membrane reactors are applied to the reactions such as dehydration and dehydrogenation, much improvement of conversion and selectivity could be accomplished.

Recently various papers on dehydrogenation in a membrane reactor appeared in the literature. Barbier *et al.* have studied methane steam reforming in a catalytic membrane reactor.<sup>6</sup> Ziaka *et al.* reported propane dehydrogenation in a high temperature membrane reactor using sol-gel alumina membrane.<sup>7</sup> Lu *et al.* studied the dehydration of 1-butanol over  $\gamma$ -Al<sub>2</sub>O<sub>3</sub> catalytic membrane reactor<sup>8</sup> and Salomon *et al.* have investigated zeolite membrane reactor for the synthesis of methyl tertiary butyl ether (MTBE).<sup>9</sup> The dehydration reaction has a problem of low yield at low temperatures. This problem can be solved by separation of water vapor by means of membrane during the reaction.

In this process, membrane plays a role in shifting thermodynamic equilibrium. In this research, ceramic membrane was prepared due to thermal stability at high temperature and compared with polymeric membranes. Also, sol-gel processes have been explored for preparing inorganic composite membrane having a microporous layer, since they allow a close control of microstructure of pores that is directly applicable to cheap and simple membrane fabrication, using either dip or spin coating procedures.<sup>10-13</sup>

Titania films have been used for a variety of dielectric applications because of its high dielectric constant and high refractive index, as well as its resistance to chemical attack. Titania is known to increase the gas permeability of the silica glass when incorporated into the glass as a glass former<sup>14</sup> and it has also been used as a constituent of porous membranes and humidity sensor because of its chemical resistance, ultra hydrophilic, photo-chemical, and catalytic properties.<sup>15-17</sup>

The purpose of this work is to develop inorganic composite membranes for the dehydration of aqueous alcohol solutions, and to investigate their permeation characteristics for penetrating molecules. Accordingly, titania was used as a top layer of the membrane, which is prepared by sol-gel method in order to promote hydrophilicity of membrane.

### Experimental Section

**Preparation of stable sols.** The colloidal silica sol was prepared by hydrolysis of tetraethyl ortho silicate (Si(OC<sub>2</sub>H<sub>5</sub>)<sub>4</sub>; TEOS, Aldrich, pure 99%). The boehmite sol (AlOOH) was

\*To whom all correspondence should be addressed. Tel: +82-42-860-7240; Fax: +82-42-861-4151; e-mail: khlee@kRICT.re.kr

obtained by hydrolysis of aluminum isopropoxide ( $\text{Al}(\text{OC}_3\text{H}_7)_3$ ; AIP, Yakuri). The sol was peptized at 90 °C by addition of mol  $\text{HNO}_3$  per mol AIP.<sup>18,19</sup> Titanium tetraisopropoxide ( $\text{Ti}(\text{OC}_3\text{H}_7)_4$ ; TIP, Aldrich, pure 99.99%) was used as precursor for the top layer. The hydrolysis of the alkoxide was carried out by addition of excess distilled water to solution of the alkoxide in ethanol. The sol was peptized at 90 °C by addition of a 0.3 mol  $\text{HCl}$  per mol TIP. The sol was vigorously stirred during the  $\text{HCl}$  addition, stirred at the same rate for 3 h thereafter. Then the sol was refluxed and stirred for 9 h. Non-supported  $\text{TiO}_2$  gel layers were produced by pouring the remaining sol-gel solutions in petri dish. The obtained gel-layers were dried at 50 °C for 24 h. Finally, the membranes were calcined for 2 h at 300 °C, 400 °C, 500 °C and 600 °C in a temperature programmable furnace. The heating and cooling rates for  $\text{TiO}_2$  membrane was 1 °C/min.

**Modification of stainless steel support.** The stainless steel disks were used to produce  $\text{TiO}_2$  composite membrane with thermal stability and mechanical stability as a porous substrate. The SUS support has a thickness of 1 mm, a diameter of 30 mm, and an average pore size of 10  $\mu\text{m}$ . To reduce the average pore size, macroporous SUS substrates were modified by packing  $\text{SiO}_2$  xerogel (500 nm) with a press under 10 Mpa and coating the intermediate layer of  $\gamma\text{-Al}_2\text{O}_3$  by soaking-rolling method as suggested by Lee and co-workers.<sup>20,21</sup> The  $\text{AlOOH}$  sols were penetrated to macropores of the first modified SUS support by suction. The modified SUS supports were dried at 25 °C and RH 60 % for 24 h, then calcined for 2 h at 650 °C. The heating and cooling rates were 1 °C/min.

**Preparation of the nanoporous top layer.**  $\text{TiO}_2$  sols were used as the material of membrane top layer and the coating procedure was the same manner as the  $\gamma\text{-Al}_2\text{O}_3$ . The preparation condition of the top layer was optimized by changing the variables. Pore size and pore size distribution were controlled by changing the calcination temperature.

**Characterization.** Several methods were used for the characterization of the membrane layers. SEM (JEOL JSM-

840A) was used to characterize the titania composite membrane. We observed the cross section, surface of the membrane and particle size of colloidal silica sols. The pore-size distribution and average pore size of the unsupported titania membrane were measured by the BET (ASAP 2010) method with argon adsorption/desorption. The structure of titania was analyzed by X-ray diffraction (XRD, D/MAX-IIIB) and gas permeation experiments were carried out in order to estimate performance of the  $\text{TiO}_2$  composite membrane

**Permeation measurements.** Permeation measurements for water/alcohol mixtures were carried out at 250 °C. The permeation apparatus is shown schematically in Figure 1. The system consists of membrane cell, furnace, temperature controller, vacuum gauge, vacuum pump and cold traps. The feed liquid was injected by syringe pump and vaporized through a heating line and the backside of membrane was evacuated through a vacuum line. The permeate vapor was collected by a cold trap cooled by liquid nitrogen. Permeation area was 4.52  $\text{cm}^2$ . The vapor permeation performance of the membrane was evaluated by permeation flux  $Q_t$  in  $\text{kg}/(\text{m}^2\cdot\text{h})$  and separation factor  $\alpha$ . The separation factor of water or methanol over organic liquid is defined as

$$\alpha_{\text{W/O}} = (y_{\text{W}}/y_{\text{O}})/(x_{\text{W}}/x_{\text{O}})$$

where  $x$  and  $y$  are the mole fractions of the water components in the binary feed mixture and in the permeate, respectively. Subscripts W and O refer to water and organic components, respectively. The mole fractions of permeate side were measured using gas chromatography (GC-14B, SHIMADZU).

## Results and Discussion

**Preparation of stable sols.** The colloidal silica and  $\text{AlOOH}$  sol were prepared as suggested by Yoldas.<sup>18</sup> The silica xerogel, was obtained by removing the solvent with a rotary evaporator. The surface morphology of the silica

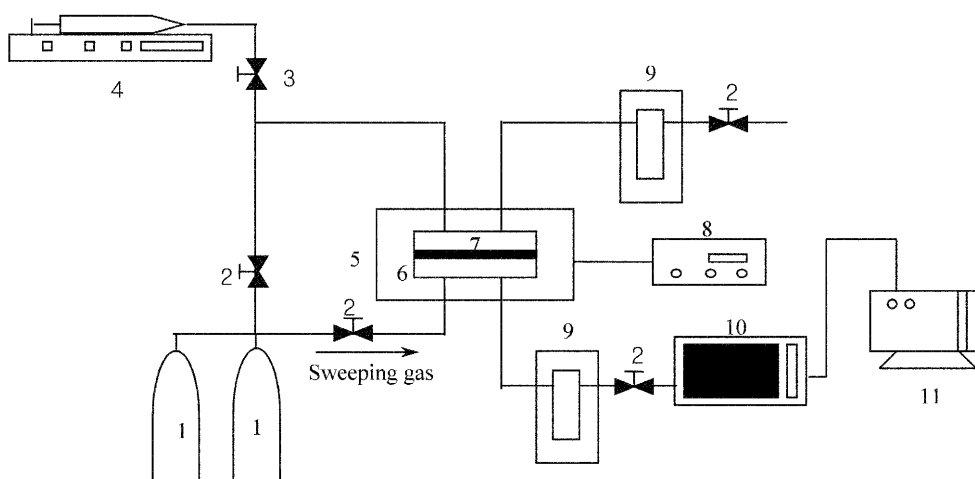


**Figure 1.** Schematic diagram of the vapor permeation apparatus. 1: Gas cylinder, 2: Ball valve, 3: Check valve, 4: Syringe pump, 5: Furnace, 6: Permeation cell, 7: Membrane, 8: Temperature controller, 9: Cold trap, 10: Gas chromatography, 11: Vacuum pump

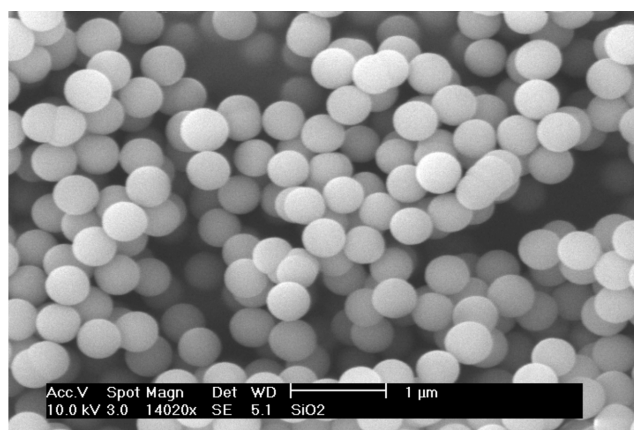


**Figure 2.** FE-SEM image of the SiO<sub>2</sub> xerogel with 500 nm-sized particles.

xerogel is shown in Figure 2. The silica xerogel was made of 500 nm-sized spherical particles. The prepared AlOOH sol was opaque blue and had the particle size of 10 nm. The unsupported  $\gamma$ -Al<sub>2</sub>O<sub>3</sub> film calcined for 2 h at 650 °C has a specific surface area of 150 m<sup>2</sup>/g, and an average pore size of 5 nm.

Titania sol was obtained *via* hydrolysis of TIP precursor under excess water, because shortage of water in the solution give rise to an unstable titania sol with the aggregation and phase separation.<sup>22</sup> The preparation condition for the stable titania sol was optimized by changing the variations. Experimental conditions for the preparation of the titania sol and structural properties of the unsupported titania film calcined at 300 °C were summarized in Tables 1 and 2. The structural properties of the unsupported titania membrane were affected by [H<sup>+</sup>]/[TIP] mole ratio. The membranes prepared with [H<sup>+</sup>]/[TIP] mole ratio larger than 0.2 have a micropore structure with an average pore size below 1.25 nm. Additionally, the corresponding adsorption/desorption isotherms

**Table 1.** Experimental conditions for the preparation of TiO<sub>2</sub> sols

Code	[H <sub>2</sub> O]/[TIP]	[H <sup>+</sup> ]/[TIP]	Catalyst	Solvent
A	100	0.3	HCl	Et-OH
B	100	0.2	HCl	Et-OH
C	100	0.1	HCl	Et-OH
D	100	0.3	HCl	Pr-OH
E	100	0.2	HCl	Pr-OH
F	100	0.1	HCl	Pr-OH

**Table 2.** Structural characteristics of TiO<sub>2</sub> films calcined at 300 °C

Code	Mean pore size (nm)	Surface area (m <sup>2</sup> g <sup>-1</sup> )	Pore volume (mL g <sup>-1</sup> )	Isotherm (type)
A	1.25	210	0.13	I
B	2.9	114	0.13	IV
C	3.2	110	0.11	IV
D	1.6	200	0.11	I
E	3.0	110	0.11	IV
F	3.2	94	0.1	IV

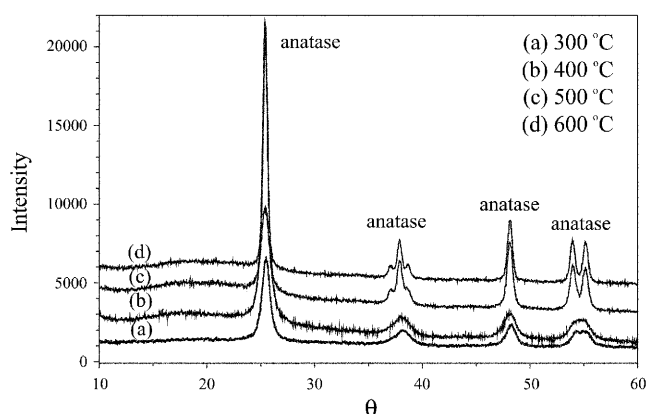


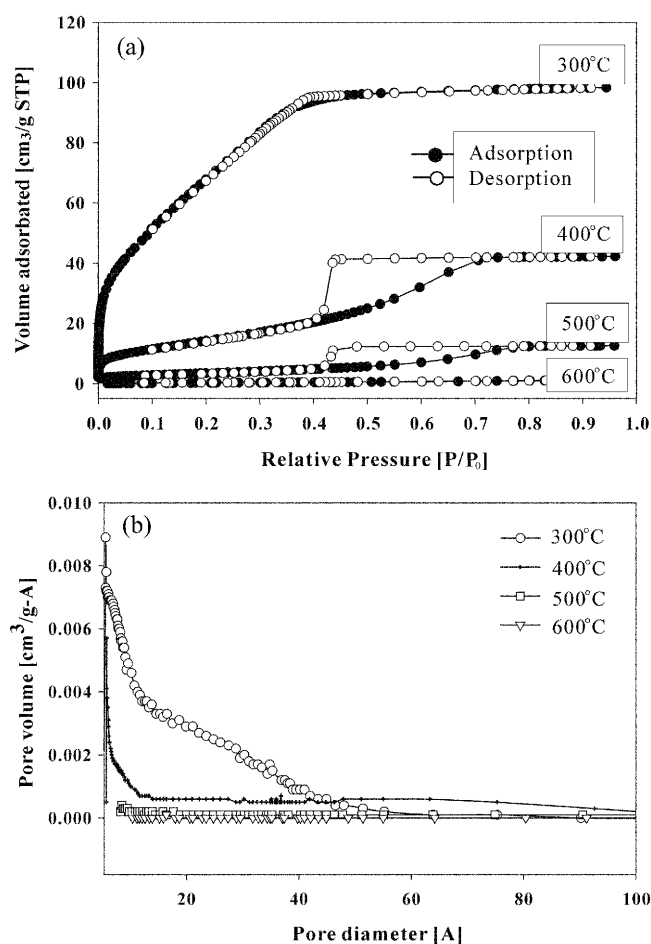
**Figure 3.** XRD patterns of the unsupported TiO<sub>2</sub> membranes calcined at various Temperatures.

were found to be type being typical for a porous material with a mainly microporous texture but the shape of the isotherms of the membranes produced with [H<sup>+</sup>]/[TIP] mole ratio less than 0.3 showed type IV. Therefore, The titania sol prepared with 0.3 of [H<sup>+</sup>]/[TIP] mole ratio and ethanol as a cosolvent is considered to be a suitable material for a toplayer.

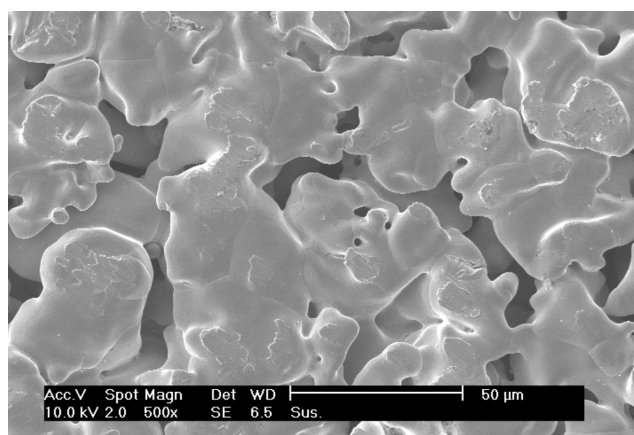
It is well-known that the calcination temperature of the membrane is higher than the operation temperature of membrane reactor. Therefore, the minimum calcination temperature is about 300 °C where the anatase phase of titania with chemical stability is formed.<sup>23</sup> To estimate the proper calcinations temperature where the qualified properties such as the pore size distribution and the specific surface area could be obtained, the films of titania were prepared at different calcinations temperatures from 300 °C to 600 °C. Figure 3 shows the results of XRD analysis for those membranes. The XRD analysis revealed that no trace of rutile phase was detected and all of the signals as shown in Figure 3 were all characteristics of the anatase phase. It means that the titania membranes prepared by sol-gel have the chemical stability.

Figure 4 shows isotherm plot and pore size distribution of the titania top layer material as a function of calcination temperatures. After thermal treatment at 300 °C, isotherm shape corresponded to type I, which is representative for microporous structures. With an increase in temperature, grain growth due to sintering resulted in a decrease in the micropore volume and surface area, and a gradual increase in the average pore size. This implies that the preparation of a stable sol-gel derived top layer maintaining the fine pore properties was feasible with thermal treatment at low temperature.

**Characterization of the TiO<sub>2</sub> composite membranes.** A porous stainless steel (SUS) was used as a support of the titania composite membrane. A top surface of the SUS support is shown in Figure 5. As shown in Figure 5, macropore above 10 nm and a very rough surface were observed. First, SUS supports were modified using silica xerogel of 500 nm-sized in order to reduce pore size and surface roughness of the SUS support. Figure 6 shows a



**Figure 4.** Isotherm plot (a) and pore size distribution (b) of unsupported TiO<sub>2</sub> membranes.



**Figure 5.** FE-SEM image of the top surface of SUS support before the modification.

SEM image of the SUS support modified by silica xerogel. Pore size and surface roughness of the SUS support were definitely reduced. SiO<sub>2</sub>/SUS support was modified again with AlOOH sols by soaking-rolling method. A SEM image of the support modified with AlOOH sols is shown in Figure 7. Modification with AlOOH sols had the pore size of the SiO<sub>2</sub>/SUS support reduced more due to penetration of

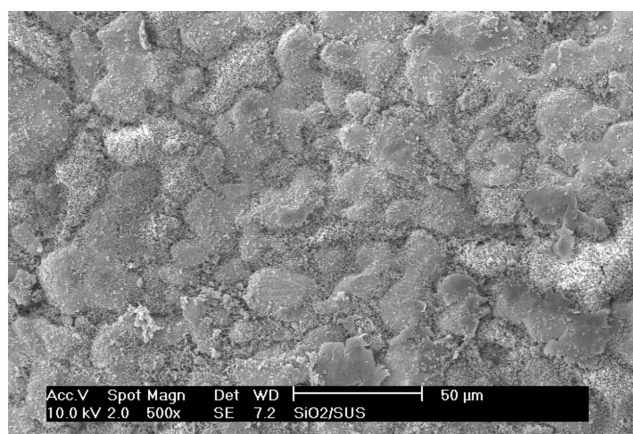
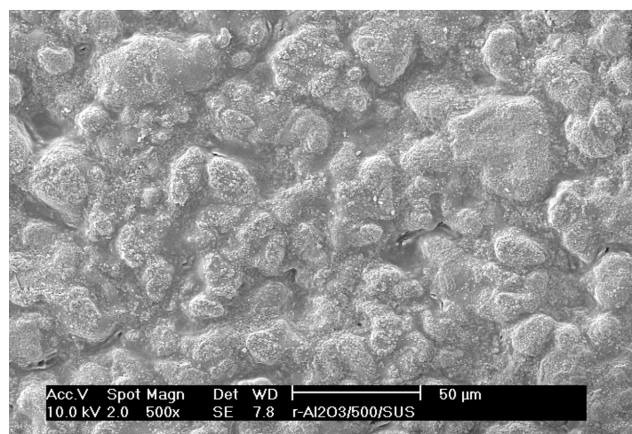
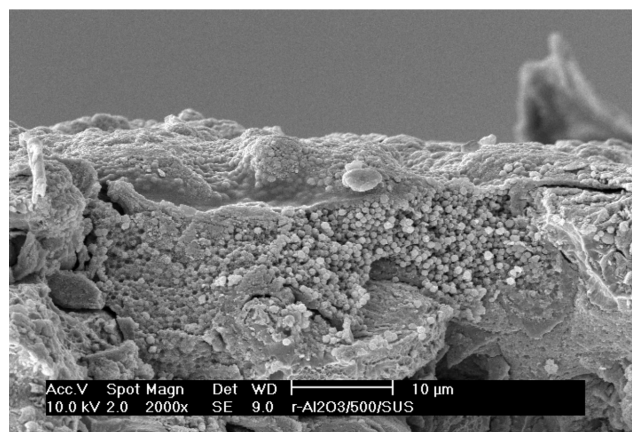


**Figure 6.** FE-SEM image of the top surface of SiO<sub>2</sub>(500 nm)/SUS support.



(a)



(b)

**Figure 7.** FE-SEM image of the (a) top surface and (b) cross-section of γ-Al<sub>2</sub>O<sub>3</sub>/SiO<sub>2</sub>(500 nm)/SUS support by modification.

AlOOH sols into the macropores of the modified SUS support with silica xerogels. The SiO<sub>2</sub>(500 nm) particles are surrounded by the γ-Al<sub>2</sub>O<sub>3</sub>. To investigate the performance of the γ-Al<sub>2</sub>O<sub>3</sub>/SiO<sub>2</sub>(500 nm)/SUS support, the nitrogen permeance was tested with a different temperature and pressure. The result is shown in Figure 8. There is a decrease

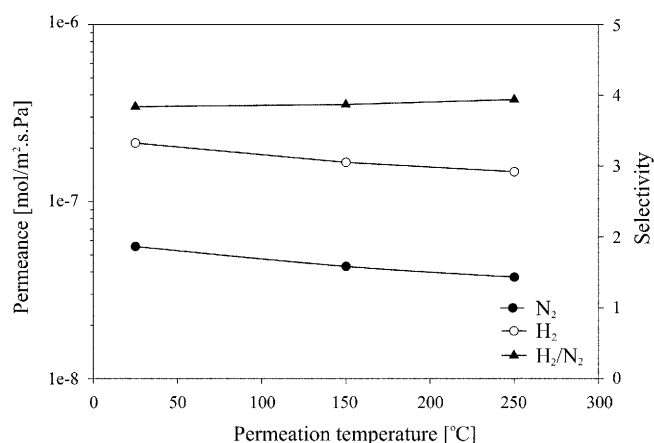
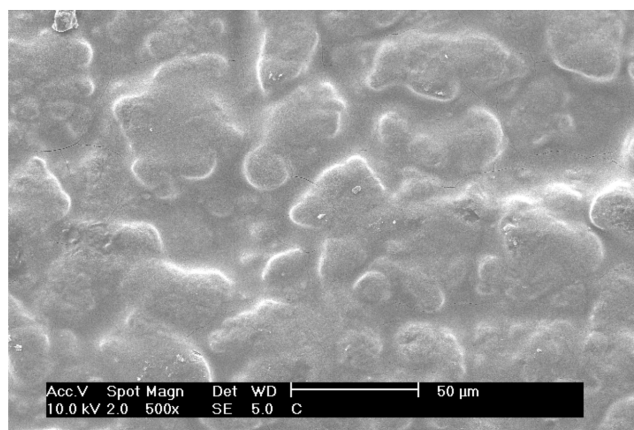


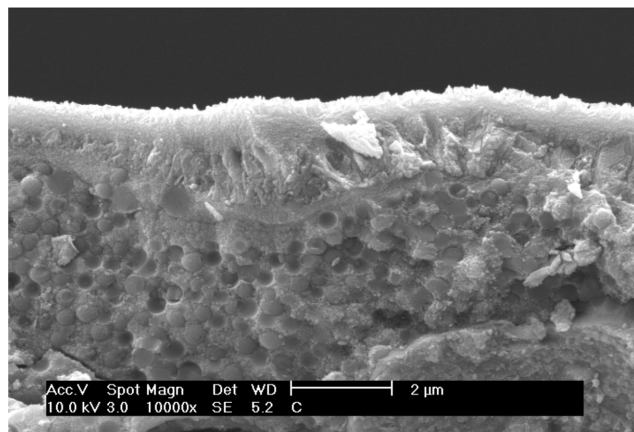
**Figure 8.** Permeance of the  $\gamma$ -Al<sub>2</sub>O<sub>3</sub>/SiO<sub>2</sub> support as a function of permeation temperature.

of nitrogen permeance with increasing permeation temperature, and the nitrogen permeance was nearly constant with increasing pressure difference. It means that the contribution of Knudsen diffusion increases by modification with  $\gamma$ -Al<sub>2</sub>O<sub>3</sub> and the  $\gamma$ -Al<sub>2</sub>O<sub>3</sub>/SiO<sub>2</sub>(500 nm)/SUS support is suitable for producing a stable titania top layer.

Titania sol as a top layer material was prepared under acid-



(a)



(b)

**Figure 9.** FE-SEM image top surface (a) and cross-section (b) of the TiO<sub>2</sub> composite membrane.

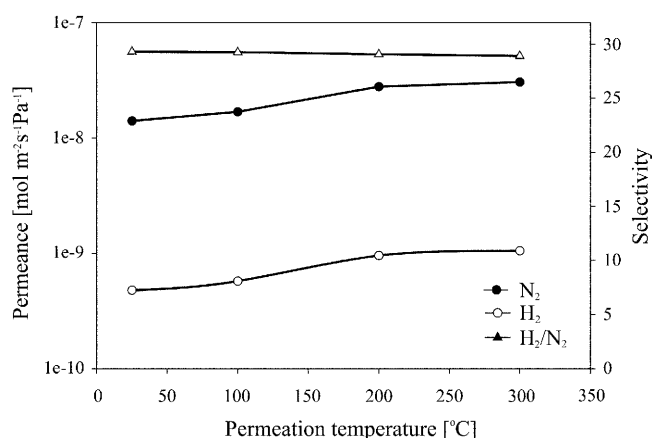


**Figure 10.** Permeance of the TiO<sub>2</sub> composite membrane as a function of permeation temperature.

catalyzed conditions. The top layer of the titania membrane was coated on the  $\gamma$ -Al<sub>2</sub>O<sub>3</sub>/SiO<sub>2</sub>(500 nm)/SUS support by soaking-rolling method of several times. Figure 9 shows SEM images of the titania top layer prepared by soaking-rolling method. Titania top layer is 1 mm thick, and its top surface has defect-free morphology. To estimate performance

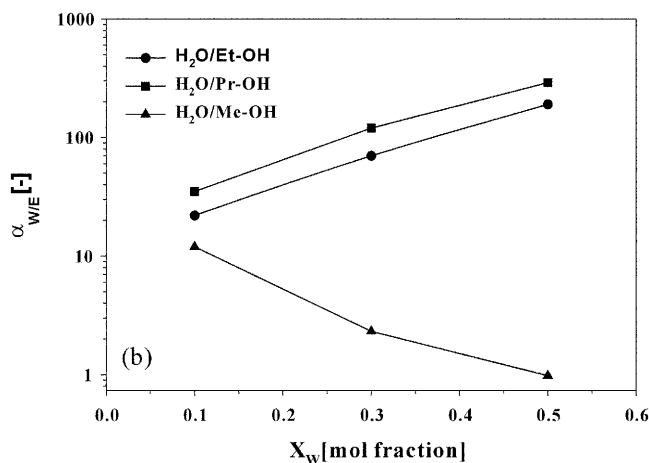
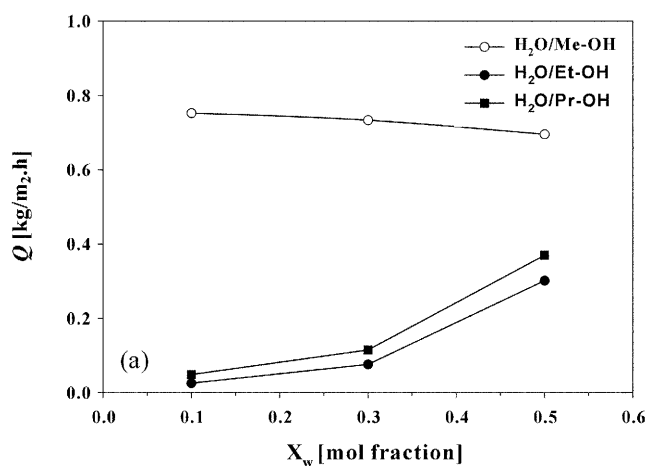


**Figure 11.** Feed composition dependence of (a) flux and (b) selectivity in vapor permeation of water/alcohol mixture for the titania membrane at 523 K.

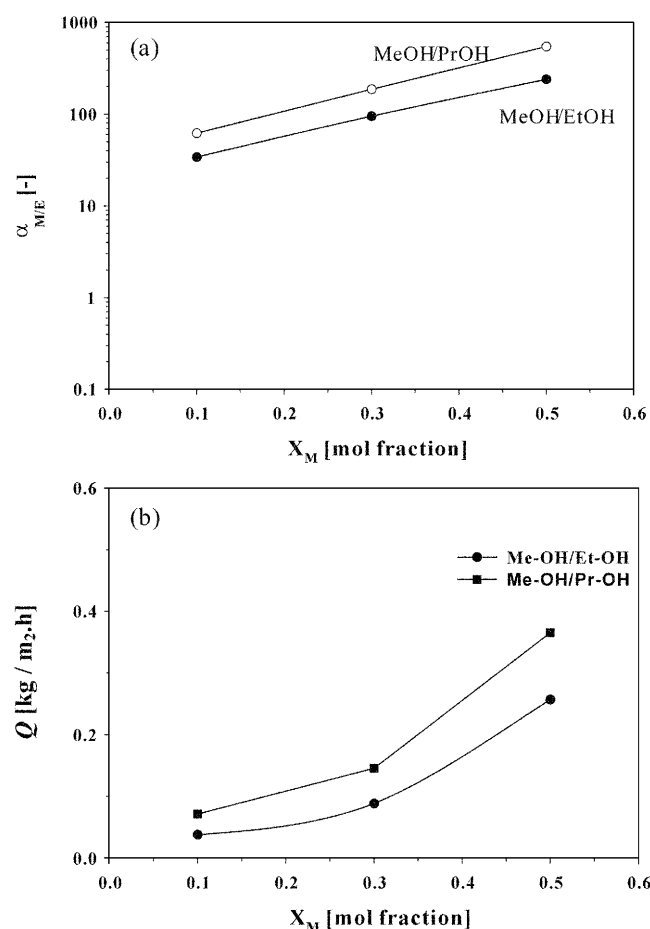


**Figure 12.** Feed composition dependence of (a) flux and (b) selectivity in vapor permeation of alcohol mixture for the titania membrane at 523 K.

of the titania composite membrane, permeation measurements for a single gas were made with the gases  $\text{N}_2$ ,  $\text{H}_2$

**Table 3.** Pore structure characteristics of  $\text{TiO}_2$  film (code A) as a function of calcination temperature

Temperature (°C)	Mean pore size (nm)	Surface area ( $\text{m}^2 \text{g}^{-1}$ )	Pore volume ( $\text{mL g}^{-1}$ )	Isotherm (type)
300	1.3	210	0.13	I
400	3.8	40	0.05	VI
500	4.3	0.92	0.015	VI
600	5.4	0.77	0.001	II

between room temperature and 250 °C. As shown in Figure 10,  $\text{H}_2$  and  $\text{N}_2$  permeances increase with increasing permeation temperature, and single gas selectivity of  $\text{H}_2/\text{N}_2$  is varied from 25 to 30. The temperature dependence of the permeance indicates that the gas permeation behavior through the titania composite membrane prepared on  $\gamma\text{-Al}_2\text{O}_3/\text{SiO}_2/\text{SUS}$  with Knudsen diffusion was dominated by activated diffusion.

**Vapor permeation characteristics of the prepared membrane.** The vapor permeation results of the titania composite membrane for various water-alcohol mixtures, methanol-ethanol mixtures and methanol-propanol mixtures appeared to Figures 11 and 12. In the case of water-alcohol mixtures, the permeation characteristics of the prepared membranes were dependent on the content and alkyl chain's length of alcohol in the feed. That is, the perm-selectivity for water molecule increased gradually with increasing the difference of molecular size and polarity between water and alcohol as showed in Table 4. Also, due to the hydrophilic property of the titania membrane, the overall performance for feed compositions is improved more according to water content in the feed. However, the effect of feed composition on the water-methanol mixtures showed a permeation behavior contradictory to overall separation trends of water-ethanol, 2-propanol mixtures. It probably seems as results that the retention time of methanol molecule by interacting

**Table 4.** Physicochemical properties of permeants

Name	water	methanol	ethanol	2-propanol
Property				
Interatomic distance (Å)	(1a-1b) : 1.52 (O1-1b) : 0.96	(2a-1a) : 2.83 (2b-2a) : 1.80	(3c-1a) : 4.05 (3b-2b) : 3.06	(4b-3c) : 4.30 (1a-3b) : 3.87
M.W. (g/mol)	18.02	32.04	46.07	60.10
Molecular volume ( $\text{cm}^3/\text{mol}$ )	11.22	21.672	31.61	41.56
Surface area ( $\text{cm}^2/\text{mol} \times 10^9$ )	2.18	3.62	4.96	6.31
Solubility parameter ( $\text{J}^{1/2}/\text{cm}^{2/3}$ )	47.80	29.61	26.50	23.51
Dispersion ( $\text{J}^{1/2}/\text{cm}^{2/3}$ )	15.60	15.11	15.76	15.76
Hydrogen bonding ( $\text{J}^{1/2}/\text{cm}^{2/3}$ )	42.30	22.31	19.39	16.34
Polarity ( $\text{J}^{1/2}/\text{cm}^{2/3}$ )	16.00	12.29	8.80	6.12
Hydrophilic surface ( $\text{cm}^2/\text{mol} \times 10^9$ )	100.00	60.88	38.02	22.02
Dipole moment ( $\mu$ )	2.00	1.65	1.61	1.67

with membrane at diffusion step was short relatively comparing to ethanol and 2-propanol. This is due to physicochemical properties of methanol molecule such as hydrophilicity and hydrogen bonding ability as can be seen in Table 4. Accordingly, it can be considered that methanol is permeated more preferentially than water, and the overall performance for feed composition also decreased with increasing water content in the feed gradually. To confirm this result, individual vapor permeation experiments for water and methanol was carried out, and a high permeation rate of methanol than water was observed (water: 603 g/m<sup>2</sup>·h, methanol : 795 g/m<sup>2</sup>·h).

In other hand, the overall performance for methanol-ethanol, 2-propanol mixtures showed trends similar to permeation behaviors of water-ethanol, 2-propanol mixtures of Figure 11, and exhibited more effective results than their mixtures. As it were, the permeation rates of methanol in mixtures consisted of methanol-ethanol and 2-propanol were higher than that of water in water-ethanol and 2-propanol mixtures, and in consequence, most of separation factors on the feed composition appeared to be good relatively, as showed in Figure 12. From the above results, it was found that the chemical affinity, hydrophilicity in this case, related to retention time of permeants in membrane plays a key role in perm-selectivity of membrane for organic matters of similar physicochemical properties.

### Conclusions

The titania sol of nanoparticles was synthesized by hydrolysis of metal alkoxide using the sol-gel process, and the composite type membranes have been prepared by calcining the coated layer at 300 °C after drying and soaking-rolling the sol upon the support membrane having a multi-layered structure composed of SiO<sub>2</sub> and  $\gamma$ -Al<sub>2</sub>O<sub>3</sub>. The microporous composite membrane exhibited the activated diffusion. For the vapor permeation of water and alcohol mixture, the prepared membranes showed the excellent water-permselective performance in most solution except water-methanol mixtures. In the methanol-alcohol mixtures, the selectivity and permeability of the membrane were dependent on the molecular size, the polarity and the hydrophilic surface of permeant organics. On the other hand, the methanol aqueous solution exhibited different permeation tendency with other feed solutions. It probably seems as results that the retention time of methanol molecule by interacting with membrane at diffusion step was short relatively comparing to water, ethanol and 2-propanol. This is due to physicochemical properties of methanol molecule

such as hydrophilicity and hydrogen bonding ability. In conclusion, we expect that the titania/alumina composite membrane is applicable to the dehydration process of alcohol mixtures at elevated temperatures.

**Acknowledgement.** This work was supported by the national research laboratory (NRL) and carbon dioxide reduction and sequestration (CDRS) programs funding from the ministry of science and technology, Korea.

### References

1. De Lange, R. S. A.; Keizer, K.; Hekkink, J. H. A.; Burggraaf, A. J. *J. Membr. Sci.* **1995**, 99, 57.
2. Tsapatsis, M.; Gavalas, G. *J. Membr. Sci.* **1994**, 87, 281.
3. Wu, J. C. S.; Sabol, H.; Smith, G. W.; Flowers, D. L.; Liu, P. K. T. *J. Membr. Sci.* **1994**, 96, 227.
4. Shelekhin, A. B.; Dixon, A. G.; Ma, Y. H. *J. Membr. Sci.* **1992**, 75, 233.
5. Zaspalis, V. T.; Keizer, K.; Ross, J. R. H.; Burggraaf, A. J. *Key Eng. Mater.* **1991**, 205, 61.
6. Barbieri, G.; Violante, V.; Di Maio, F. P.; Criscuoli, A.; Drioli, E. *Ind. Eng. Chem. Res.* **1997**, 36, 3369.
7. Ziaka, Z. D.; Minet, R. G.; Tsotsis, T. T. *J. Membr. Sci.* **1993**, 77, 221.
8. Lu, M.; Xiong, G.; Zhao, H.; Cui, W.; Gu, J.; Bauser, H. *Catalysis Today* **1995**, 25, 339.
9. Salomon, M. A.; Coronas, J.; Menendez, M.; Santamiria, J. *Applied Catalysis A. General* **2000**, 200, 201.
10. Gouma, P. I.; Dutta, P. K.; Mills, M. J. *NanoStructured Materials* **1999**, 11, 1231.
11. Venza, P. A.; Frosta, R. L.; Bartlett, J. R.; Woolfrey, J. L.; Klopoggea, J. T. *Thermochimica Acta* **2000**, 346, 73.
12. Ahonen, P. P.; Richard, O.; Kauppinen, E. I. *Materials Research Bulletin* **2001**, 36, 2017.
13. Suh, D.-J.; Park, T.-J. *Chem. Mater.* **1996**, 8, 509.
14. Shelby, J. E. *J. Am. Ceram. Soc.* **1972**, 55, 195.
15. Anderson, M. A.; Gieselman, M. J.; Xu, Q. *J. Membr. Sci.* **1988**, 39, 243.
16. Zaspalis, V. T.; Keizer, K.; Van Praag, W.; Van Ommen, J. G.; Ross, J. R. H.; Burggraaf, A. J. *Br. Ceram. Proc.* **1988**, 43, 103.
17. Traversa, E.; Gnappi, G.; Montenero, A.; Gusmano, G. *Sensors & Actuators B* **1996**, 31, 59.
18. Brinker and Scherer *Sol-Gel Science*; Academic Press: 1990; p 273.
19. Sea, B.; Lee, K.-H. *Bull. Korean Chem. Soc.* **2001**, 22, 1400.
20. Lee, K.-H.; Lee, D.-W.; Lee, Y.-G.; Sea, B. K. *Korea Patent* 2002-0060554, 2002.
21. Lee, D.-W.; Lee, Y.-G.; Ihm, S.-K.; Lee, K.-H. *Langmuir* **2003**, Submitted.
22. So, W.-W. *Ph. D. thesis*, Korea Advanced Institute Science and Technology: Korea, 1998.
23. Gestel, T. V.; Vandecasteele, C.; Buekenhoudt, A.; Dotremont, C.; Luyten, J.; Leysen, R.; Der Bruggen, B. B.; Maes, G. *J. Membr. Sci.* **2002**, 207, 73.